East African Scholars Journal of Engineering and Computer Sciences OPEN ACCESS
Abbreviated Key Title: East African Scholars J Eng Comput Sci
ISSN: 2617-4480 (Print) & ISSN: 2663-0346 (Online)
Published By East African Scholars Publisher, Kenya

Volume-3 | Issue-5 | May-2020 | DOI: 10.36349/easjecs.2020.v03i05.001

Research Article

Similarity Analysis of Mass and Heat Transfer of FHD Steady Flow of Nanofluid Incorporating Magnetite Nanoparticles (Fe3O4)

A.S. Rashed*[1], E.H. Nasr[2] and M.M. Kassem[1]

[1]Department of Physics and Engineering Mathematics, Faculty of Engineering, Zagazig university, Egypt
[2]Delta Higher Institute for Engineering and Technology, Mansoura, Egypt

Article History
Received: 18.04.2020
Accepted: 25.05.2020
Published: 28.05.2020

Journal homepage:
https://www.easpublisher.com/easjecs

Quick Response Code

Abstract: Similarity analysis was created to study the properties of heat and mass transfer of ferro hydro dynamic (FHD) of steady nanofluid flow incorporating magnetite (Fe3O4) nanoparticles. A variable magnetic source is located at the end of a vertical plate immersed in the fluid which is responsible for generating the magnetic field affecting the FHD flow. The group method was employed to remodel the governing system into an ordinary differential equation system. The recent research was inspired by examining the effect of three parameters, including the volume fraction of nanoparticles ϕ, the magnetic field strength of the source γ, and the ambient temperature difference ratio 〖 γ〗 _T. The results showed that both velocity components decrease inside the boundary layer when ϕ and γ_T increase and slightly increase when γ values increase. The shear stress and temperature distribution of the fluid inside the layer decrease when ϕ increases while both increase when the other parameters increase. On the other hand, the heat flux increases only when ϕ values increase.

Keywords: Ferro-hydrodynamic; Nanofluids, Group Method.

INTRODUCTION

Nanofluid, a name coined by Dr.choi at the Argonne National Laboratory to describe a fluid consisting of solid nanoparticles with a size of less than 100 nm suspended on it, usually with solid volume fractions of less than 4%. Nanofluids are synthesized by metal and metal oxides suspended nanoparticles. The word "nanomaterials" includes a broad variety of materials, including nanocrystalline materials, nanocomposites, nanotubes of carbon, and quantum dots (Pal, S. *et al.*, 2011). Described the thermomagnetic based ferrofluid to develop microfluidic applications. Aminfar, H. *et al.*, (2012) studied hydrothermal simulation of the two-phase model conducting an electrically conductive ferrofluid Sheikholeslami, M., & Ganji, D. D. (2014). Studied the effects induced by ferrohydrodynamic and magnetohydrodynamic flows on ferrofluid flow and heat transfer (Ghasemian, M. *et al.*, 2015) studied the heat transfer features of Fe_2O_3 ferrofluid flowing under alternating and constant magnetic fields using a mini-channel model (Sheikholeslami, M. *et al.*, 2015). Used a magnetic source to show heat transfer and ferrofluid flow in a semi-annulus domain as thermal radiation. In (Majeed, A. *et al.*, 2016) the authors studied the effect of a variable magnetic field to show the forced convection Majeed, A. *et al.*, (2016). In the presence of a dipole and a prescribed heat flux, studied heat transfer and unsteady ferromagnetic liquid flow over a stretch sheet Goshayeshi, H. R. *et al.*, (2016). Used pulsating heat pipe to research the effect of particle size and form on ferro-nanofluid heat transfer Sun, X. H. *et al.*, (2019) studied the transfer of isotropic heat and natural convection in the presence of a magnetic field in a ferro-nanofluid. Monroe *et al.*, (2019) studied the ability of a ferro-nanofluid to pass heat within pipes.

Several approaches have been employed to study different applications of fluid dynamics and evolutionary equations that model ocean and shallow water waves. These methods include finite volume (Ghasemian, M. *et al.*, 2015; Sharifi, A. *et al.*, 2019; & Nessab, W. *et al.*, 2019), control volume based finite element method (Aminfar, H. *et al.*, 2012; Sheikholeslami, M., & Ganji, D. D. 2014; Sheikholeslami, M. *et al.*, 2015; & Sheikholeslami, M. *et al.*, 2016), incompressible Smoothed Particles Hydrodynamics (ISPH) method (Aly, A. M., & Ahmed, S. E. 2020), group transformation and Lie symmetry methods (Mabrouk, S. M., & Rashed, A. S. 2017; Rashed, A. S. 2019; Saleh, R. *et al.*, 2017; Rashed, A. S., & Kassem, M. M. 2008; Mabrouk, S., & Kassem, M. 2014; Mabrouk, S. *et al.*, 2013; Kassem, M. M., &

Rashed, A. S. 2009; Kassem, M. M., & Rashed, A. S. 2019; & Mabrouk, S. M., & Rashed, A. S. 2019).

The main purpose of this work is to research the effect of a magnetic source on ferro-nanofluid incorporating iron oxide (Fe_3O_4) nanoparticles with water as a base fluid. To reduce the complexity of the governing equations into a simpler type of ordinary differential equations (ODEs), a precise transformation technique was developed. The numerical calculations have been carried out for three significant parameters including nanoparticles volume fraction, $\emptyset$, magnetic field strength of the magnetic source, γ and temperature difference ratio with respect to ambient temperature, $\gamma_T = \frac{\Delta T}{T_\infty}$.

MATHEMATICAL FORMULATION

Let the nanofluid flow to be, steady, laminar, subjected to constant pressure in two dimensions. The governing equations describe the flow adjacent to a vertical plate in the presence of an originally placed magnetic source, as shown in Fig. 1. This case is mathematically modeled including the magnetization effect and neglecting both of induced Lorentz forces and diffusion in x-direction. This can be implemented in the form:

$$\frac{\partial u}{\partial x} + \frac{\partial v^*}{\partial y} = 0 \quad \textbf{(2.1)}$$

$$u\frac{\partial u}{\partial x} + v^*\frac{\partial u}{\partial y} = \upsilon_{nf}\left[\frac{\partial^2 u}{\partial y^2}\right] + \frac{\mu_0 M}{\rho_{nf}}\frac{\partial H}{\partial x} \quad \textbf{(2.2)} \qquad (2.2)$$

$$u\frac{\partial T}{\partial x} + v^*\frac{\partial T}{\partial y} = \alpha_{nf}\left[\frac{\partial^2 T}{\partial y^2}\right] \quad \textbf{(2.3)} \qquad (2.3)$$

Where adjacent plate temperature isT_w and external boundary layer is T_∞, ν kinematic viscosity, k denotes permeability, α is the thermal diffusivity and T the distribution of temperature within the layer and the subscript, nf, refers to nanofluid properties.

The plate undergoes the following conditions:

$$u(x,0) = u_w(x), u(x,\infty) = 0, v^*(x,0) = v_w(x), T(x,0) = T_w, T(x,\infty) = T_\infty \quad \textbf{(2.4)}$$

The source's magnetic potential is defined here by:

$$\epsilon(x,y) = -\frac{\gamma}{2\pi}\left(\tan^{-1}\left(\frac{y}{x}\right)\right) \quad \textbf{(2.5)}$$

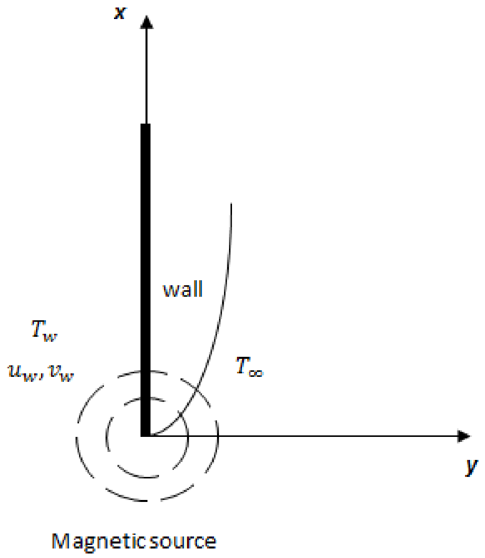

Fig. 1 Physical model of the problem

Now, components of the magnetic field in the x and y directions are given by:

$$H^x = -\frac{\partial \epsilon}{\partial x} = -\frac{\gamma}{2\pi}\left(\frac{y}{(\square)^2 + (y)^2}\right) \quad \textbf{(2.6)}$$

$$H^y = -\frac{\partial \epsilon}{\partial y} = \frac{\gamma}{2\pi}\left(\frac{x}{(x)^2 + (y)^2}\right) \quad \textbf{(2.7)}$$

And the magnetic flux total is determined by:

$$\bar{H} = \sqrt{(H^x)^2 + (H^y)^2} = \frac{\gamma}{2\pi}\left(\frac{1}{\sqrt{x^2+y^2}}\right) \quad \textbf{(2.8)}$$

The magnetization, M, and the components of the induced magnetic field, B^x and B^y, are given by:

$$M = kH(T_c - T), B^x = \mu_0 H^x \text{ and } B^y = \mu_0 H^y \; (2.9)$$

Normalization process can be executed to the boundary conditions in (2.4) by:

$$U(x,y) = \frac{u(x,y)}{u_w(x)}, V(x,y) = \frac{v^*(x,y)}{v_w(x)}, \theta(x,y) = \frac{T(x,y)-T_\infty}{T_w - T_\infty} = \frac{T(x,y)-T_\infty}{\Delta T} \quad \textbf{(2.10)}$$

Equations (2.1)-(2.3) become:

$$u_w \frac{\partial U}{\partial x} + U\frac{du_w}{dx} + v_w \frac{\partial V}{\partial y} = 0 \; (2.11)$$

$$U u_w \left(U\frac{du_w}{dx} + u_w \frac{\partial U}{\partial x}\right) + V v_w u_w \frac{\partial U}{\partial y} - \upsilon_{nf}\left(u_w \frac{\partial^2 U}{\partial y^2}\right) - \frac{\mu_0 kH(T_c - T)}{\rho_{nf}}\frac{\partial H}{\partial x} = 0 \quad \textbf{(2.12)}$$

$$U u_w \Delta T \frac{\partial \theta}{\partial x} + V v_w \Delta T \frac{\partial \theta}{\partial y} - \alpha_{nf}\Delta T \frac{\partial^2 \theta}{\partial y^2} = 0 \quad \textbf{(2.13)}$$

Boundary conditions become:

$$U(x,0) = 1, V(x,0) = 1, \theta(x,0) = 1, U(x,\infty) = 0, \theta(x,\infty) = 0 \; (2.14)$$

INVARIANT GROUP TRANSFORMATION OF THE SYSTEM

A group structure of one parameter (α) is added to reduce the PDE system to an ODE system with η as the only variable of similarity.

Formulation of the problem

Consider the group structure to be in the form:

$$G: \bar{S} = K^s(\alpha)S + Q^s(\alpha) \quad (3.1)$$

Using S stands for the system variables, K^s stands for the differential coefficients function and Q^s real values. Partial derivatives become:

$$\left.\begin{aligned}\bar{S_{\bar{\imath}}} &= \left(\frac{K^s}{K^i}\right) S_i \\ \bar{S_{\bar{\imath}\bar{\jmath}}} &= \left(\frac{K^s}{K^i K^j}\right) S_{ij}\end{aligned}\right\} i = x, y \text{ and } j = x, y \quad (3.2)$$

The problem analysis

Equation (2.10) becomes:

$$\bar{u}_w \frac{\partial \bar{U}}{\partial \bar{x}} + \bar{U}\frac{d\bar{u}_w}{d\bar{x}} + \bar{v}_w \frac{\partial \bar{V}}{\partial \bar{y}} = H_1(\alpha)\left[u_w \frac{\partial U}{\partial x} + U\frac{du_w}{dx} + v_w \frac{\partial V}{\partial y}\right] \quad (3.3)$$

$H_1(\alpha)$ Stands for an equivalence parameter and slashes stands for the transformed variables. Using (3.1) and (3.2) into (3.3) leads to:

$$\left(K^U \frac{K^{u_w}}{K^x}\right) u_w \frac{\partial U}{\partial x} + \left(K^U \frac{K^{u_w}}{K^x}\right) U \frac{du_w}{dx} + \left(K^V \frac{K^{v_w}}{K^y}\right) v_w \frac{\partial V}{\partial y} = H_1(\alpha)\left[u_w \frac{\partial U}{\partial x} + U\frac{du_w}{dx} + v_w \frac{\partial V}{\partial y}\right] \quad \textbf{(3.4)}$$

Similarly, equation (2.11) becomes:

$$\bar{U}\bar{u}_w \left(\bar{U}\frac{d\bar{u}_w}{d\bar{x}} + \bar{u}_w \frac{\partial \bar{U}}{\partial \bar{x}}\right) + \bar{V}\bar{v}_w \bar{u}_w \frac{\partial \bar{U}}{\partial \bar{y}} - \upsilon_{nf}\left(\bar{u}_w \frac{\partial^2 \bar{U}}{\partial \bar{y}^2}\right) - \frac{\mu_0 kH(T_c - T)}{\rho_{nf}}\frac{\partial H}{\partial x} = H_2(\alpha)\left[U u_w \left(U\frac{du_w}{dx} + u_w \frac{\partial U}{\partial x}\right) + V v_w u_w \frac{\partial U}{\partial y} - \upsilon_{nf}\left(u_w \frac{\partial^2 U}{\partial y^2}\right) - \frac{\mu_0 kH(T_c - T)}{\rho_{nf}}\frac{\partial H}{\partial x}\right] \quad \textbf{(3.5)}$$

Using (3.1) and (3.2) into (3.5) leads to:

$$K^U K^{u_w} U u_w \left(K^U \frac{K^{u_w}}{K^x} U \frac{du_w}{dx} + K^U \frac{K^{u_w}}{K^x} u_w \frac{\partial U}{\partial x}\right) + K^U K^V \frac{K^{u_w}}{K^y} V v_w u_w \frac{\partial U}{\partial y} - \upsilon_{nf}\left(K^U \frac{K^{u_w}}{(K^y)^2} u_w \frac{\partial^2 U}{\partial y^2}\right) - \frac{\mu_0 kH(T_c - T)}{\rho_{nf}}\frac{\partial H}{\partial x} = H_2(\alpha)\left[U u_w \left(U\frac{du_w}{dx} + u_w \frac{\partial U}{\partial x}\right) + V v_w u_w \frac{\partial U}{\partial y} - \upsilon_{nf}\left(u_w \frac{\partial^2 U}{\partial y^2}\right) - \frac{\mu_0 kH(T_c - T)}{\rho_{nf}}\frac{\partial H}{\partial x}\right] \quad (3.6)$$

Similarly, equation (2.12) becomes:

$$\bar{U}\bar{u}_w \Delta T \frac{\partial \bar{\theta}}{\partial \bar{x}} + \bar{V}\bar{v}_w \Delta T \frac{\partial \bar{\theta}}{\partial \bar{y}} - \alpha_{nf}\Delta T \frac{\partial^2 \bar{\theta}}{\partial \bar{y}^2} = H_3(\alpha)\left[U u_w \Delta T \frac{\partial \theta}{\partial x} + V v_w \Delta T \frac{\partial \theta}{\partial y} - \alpha_{nf}\Delta T \frac{\partial^2 \theta}{\partial y^2}\right] \quad \textbf{(3.7)}$$

Then, using (3.1) and (3.2) into (3.7) leads to:

$$K^U \frac{K^{u_w}K^\theta}{K^x} U u_w \Delta T \frac{\partial\theta}{\partial x} + K^V \frac{K^{v_w}K^\theta}{K^y} V v_w \Delta T \frac{\partial\theta}{\partial y} - \frac{K^\theta}{\left(K^{y^2}\right)} \alpha_{nf} \Delta T \frac{\partial^2\theta}{\partial y^2} = H_3(a)[U u_w \Delta T \frac{\partial\theta}{\partial x} + V v_w \Delta T \frac{\partial\theta}{\partial y} - \alpha_{nf} \Delta T \frac{\partial^2\theta}{\partial y^2}]$$

(3.8)

Invariance condition results in:

$K^y = K^v = 1,\ K^x = K^U K^{u_w}, K^y = K^V K^{v_w}$ (3.9)

$Q^U = Q^{u_w} = Q^V = Q^{v_w} = Q^\theta = 0$ **(3.10)**

Finally, group G become:

$$G:\begin{cases} G_1 \begin{cases} \bar{x} = x + Q^x \\ \bar{y} = y + Q^y \end{cases} \\ G_2 \begin{cases} \bar{U} = \frac{K^x}{K^{u_w}} U \\ \bar{u}_w = K^{u_w} u_w \\ \bar{V} = \frac{K^y}{K^{v_w}} V \\ \bar{v}_w = K^{v_w} v_w \\ \bar{\theta} = K^\theta \theta \end{cases} \end{cases} \quad \textbf{(3.11)}$$

The complete transform of the system:

Using Morgan's theorem (Sun, X. H. et al., 2019) which states that:

$\sum_{i=1}^{6} (\gamma_i S_i + \delta_i) \frac{\partial q_i}{\partial S_i} = 0$ (3.12)

The system reduces from independent variables to one similarity variable, where dependent variables U, u_w, V, v_w, θ become invariant new similarity variables. S_i original system variables $(x, y, U, u_w, V, v_{\square}, \theta)$, q_i group transformed variables and the γ_i *and* δ_i are defined as:

$$\begin{cases} \gamma_i = \frac{\partial K^{S_i(\alpha)}}{\partial \alpha} \\ \delta_i = \frac{\partial Q^{S_i(\alpha)}}{\partial \alpha} \end{cases} \quad (3.13)$$

Transformation of the independent variables$(\mathbf{x}, \mathbf{y})$:

A single similarity variable has been obtained by applying equation (3.12) to independent variables x, y. Following the same steps in (Mabrouk, S. M., & Rashed, A. S. 2017; Saleh, R. *et al.*, 2017; Rashed, A. S., & Kassem, M. M. 2008; Mabrouk, S., & Kassem, M. 2014; Mabrouk, S. *et al.*, 2013; & Kassem, M. M., & Rashed, A. S. 2009), the variables are given by:

$\eta(x, y) = \Gamma(x) y$ (3.14)

While the dependent variables become:

$$\begin{cases} U = \omega(x) F(\eta) \\ u_w = u_w(x) \\ V = V(\eta) \\ v_w = v_w(x) \\ \theta = \theta(\eta) \end{cases} \quad \textbf{(3.15)}$$

Where $\Gamma(x), \omega(x), u_w(x)$ *and* $v_w(x)$ arbitrary functions to be evaluated during the reduction process.

Now, the system (2.11)-(2.13) becomes:

$$V' + \left[\frac{u_w \omega \Gamma^{\cdot}(x)}{v_w \Gamma^2(x)}\right] \eta F' + \left[\frac{u_w \omega^{\cdot}}{v_w \Gamma(x)}\right] F + \left[\frac{\omega \frac{du_w}{dx}}{v_w \Gamma(x)}\right] F = 0 \quad (3.16)$$

$$\left[\frac{u_w\omega\Gamma(x)}{\Gamma\cdot(x)}\right]\eta FF' + \left[\frac{u_w\omega\cdot\Gamma^2(x)}{(\Gamma\cdot(x))^2}\right]F^2 + \left[\frac{\omega\frac{du_w}{dx}\Gamma^2(x)}{(\Gamma\cdot(x))^2}\right]F^2 + \left[\frac{v_w\Gamma^3(x)}{(\Gamma\cdot(x))^2}\right]VF' = \left[\frac{\Gamma^4(x)}{(\Gamma\cdot(x))^2}\right]\upsilon_{nf}F" - \left[\frac{\Gamma^5(x)}{(\Gamma\cdot(x))^2\omega u_w}\right]\frac{\mu_0 k}{\rho_{nf}}(\Delta T_c - \Delta T\square)\frac{\gamma^2}{4\pi^2(1+\eta^2)^2} \qquad (3.17)$$

$$\left[\frac{u_w\omega\Gamma\cdot(x)}{\Gamma^3(x)}\right]\eta\theta' F + \left[\frac{v_w\Gamma(x)}{\Gamma^2(x)}\right]V\theta' = \alpha_{nf}\theta" \qquad (3.18)$$

Where $\Delta T = T_w - T_\infty, \Delta T_c = T_c - T_\infty$, we indicate derivative with respect to η by dashes. To simplify equations (3.16)-(3.18) we can use the following simplifications:

$$\begin{cases} A_1 = \frac{u_w\omega\Gamma\cdot(x)}{v_w\Gamma^2(x)} \\ A_2 = \frac{u_\square\omega\cdot}{v_w\Gamma(x)} \\ A_3 = \frac{\omega\frac{du_w}{dx}}{v_w\Gamma(x)} \end{cases} \qquad (3.19)$$

$$\begin{cases} A_4 = \frac{u_w\omega\Gamma(x)}{\Gamma\cdot(x)} \\ A_5 = \frac{u_w\omega\cdot\Gamma^2(x)}{(\Gamma\cdot(x))^2} \\ A_6 = \frac{\omega\frac{du_w}{dx}\Gamma^2(x)}{(\Gamma\cdot(x))^2} \\ A_7 = \frac{v_w\Gamma^3(x)}{(\Gamma\cdot(x))^2} \\ A_8 = \frac{\Gamma^4(x)}{(\Gamma\cdot(x))^2} \\ A_9 = \frac{\Gamma^5(x)}{(\Gamma\cdot(x))^2\omega u_w} \end{cases} \qquad (3.20)$$

$$\begin{cases} A_{10} = \frac{u_w\omega\Gamma\cdot(x)}{\Gamma^3(x)} \\ A_{11} = \frac{v_w\Gamma(x)}{\Gamma^2(x)} \end{cases} \qquad (3.21)$$

In order to ensure that equations (3.16)-(3.18) are ODE, the A's values must be either functions of η or constants.

We Can Get The Following Results From Analysis:

$$\Gamma(x) = \frac{1}{x}, \eta(x,y) = \frac{y}{x}, u_w(x) = 1, \omega(x) = \frac{1}{x}, v_w = \frac{1}{x} \qquad (3.22)$$

So

$$\begin{cases} A_1 = -1 \\ A_2 = -1 \\ A_3 = 0 \\ A_4 = -1 \\ A_5 = -1 \\ A_6 = 0 \\ A_7 = 1 \\ A_8 = 1 \\ A_9 = 1 \\ A_{10} = -1 \\ A_{11} = 1 \end{cases} \quad (3.23)$$

The final form of ODE system becomes:

$$V' - \eta F' - F = 0 \quad (3.24)$$

$$-\eta F F' - F^2 + V F' = \upsilon_{nf} F'' - \frac{\mu_0 k}{\rho} (\Delta T_c - \Delta T \theta) \frac{\gamma^2}{4\pi^2 (1+\eta^2)^2} \quad (3.25)$$

$$-\eta \theta' F + V \theta' = \alpha_{nf} \theta'' \quad (3.26)$$

subjected to the boundary conditions described by (2.14).

where the nanofluid parameters are calculated by the following relations relative to the properties of base fluid, nanoparticles properties and volumetric fraction of nanoparticles addition.

$$\left(\rho C_p\right)_{nf} = \left(\rho C_p\right)_f (1 - \phi) + \left(\rho C_p\right)_s \phi \quad (3.27)$$

$$k_{nf} = \left(\frac{k_s + 2k_f - 2\phi(k_f - k_s)}{k_s + 2k_f + \phi(k_f - k_s)}\right) k_f \quad (3.28)$$

$$\mu_{nf} = \frac{\mu_f}{(1-\phi)^{2.5}} \quad (3.29)$$

$$\sigma_{nf} = \left(1 + \frac{3\left(\frac{\sigma_s}{\sigma_f} - 1\right)\phi}{\left(\frac{\sigma_s}{\sigma_f} + 2\right) - \left(\frac{\sigma_s}{\sigma_f} - 1\right)\phi}\right) \sigma_f \quad (3.30)$$

RESULTS AND DISCUSSION

The equations, (3.24)-(3.26), subjected to boundary conditions, (2.14) have been solved numerically using Runge-Kutta method in order to study the effects of the three parameters under consideration.

Effect of nanoparticles volumetric fraction, $\emptyset$

The findings indicate that growing volume corresponds to a strong decrease in all ferrofluid velocity elements, as nanoparticles form barriers in the flow of fluid. A significant drop in shear stress and temperature distribution is also observed. At the other hand, the heat flux within the boundary layer decreases. These findings are shown and demonstrated in Figs. 2-5.

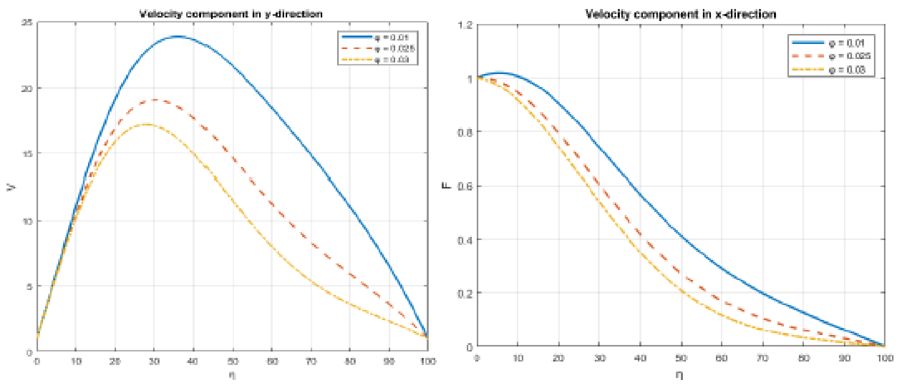

Fig. 2 Effect of volumetric fraction,ϕ ,on velocity components in both directions.

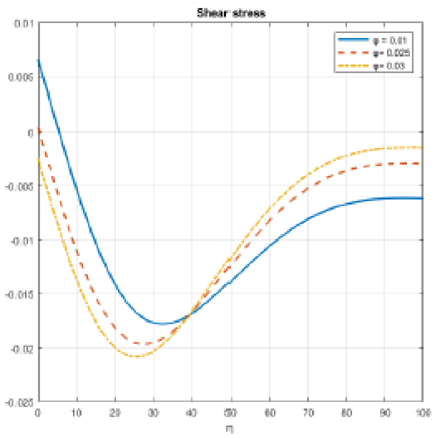

Fig.3 Effect of ϕ on Shear stress

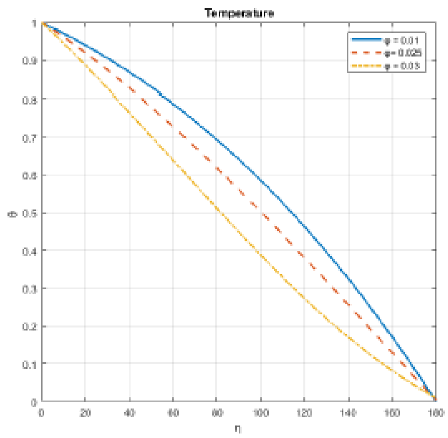

Fig.4 Effect of ϕ on temperature

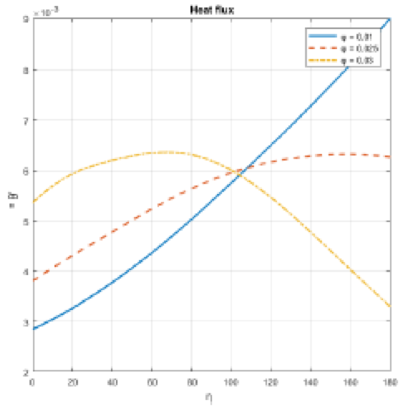

Fig. 5. Effect of ϕ on heat flux

Effect of magnetic field strength of the source γ

The difference of the magnetic source power has a noticeable effect on the temperature and heat flow inside the layer. This has a minor impact on all nanofluid velocity components and shear stress. All are raised due to a rise in magnetic source power as seen in Figs. 7-11.

Effect of temperature difference ratio with respect to ambient temperature γ_T

Moreover, the results show that increasing temperature difference ratio with respect to ambient temperature, γ_T, leads to a corresponding increase in flow velocity, shear stress and temperature distribution. On the contrarily, the heat flux is decreased as illustrated as illustrated in Figs. 12-16.

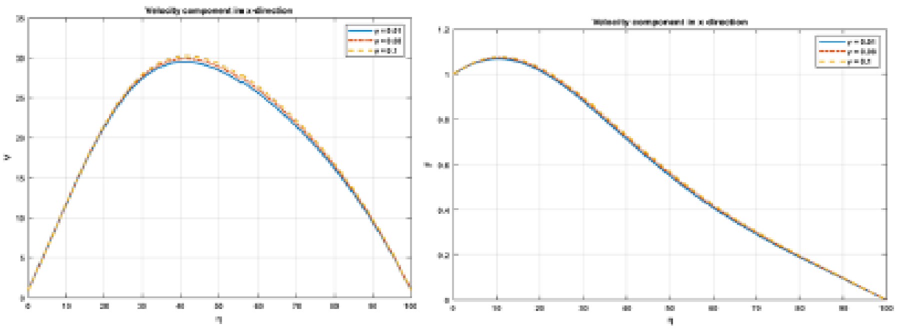

Fig. 7. Effect of magnetic field strength,γ ,on velocity components in both directions

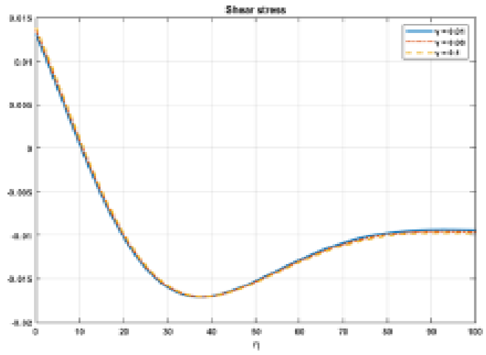

Fig. 8 Effect of γ on shear stress

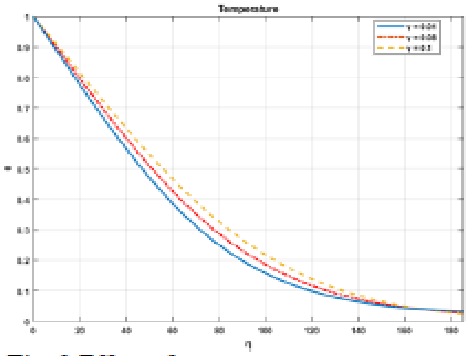

Fig. 9 Effect of γ on temperature

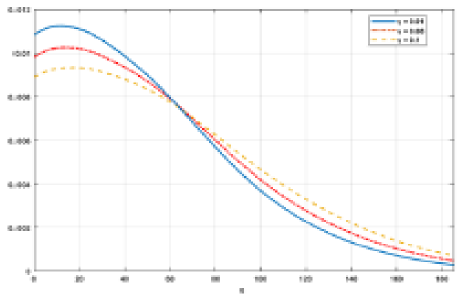

Fig. 10 Effect of γ on heat flux

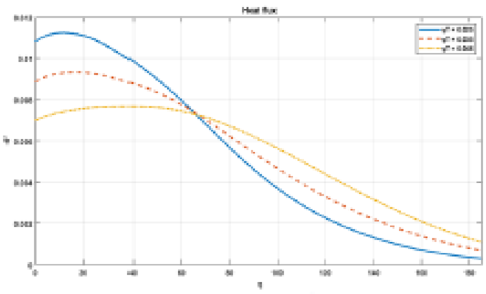

Fig. 11 Effect of γ_T on heat flux

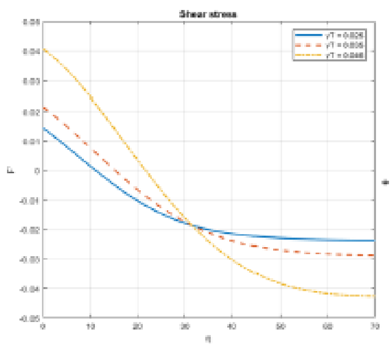

Fig. 13. Effect of γ_T on Shear stress

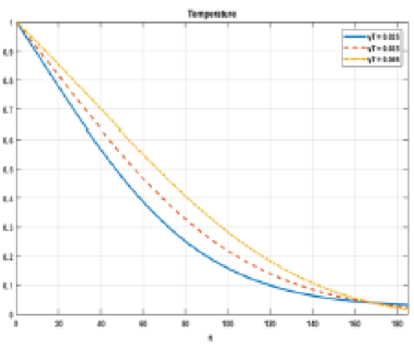

Fig. 14. Effect of γ_T on temperature

CONCLUSIONS

The effect of a variable strength magnetic source on the ferro nanofluid flow adjacent to a vertical plate has been studied. The nanofluid consists of water, a base fluid that contains magnetite iron oxide (Fe_3o_4) nanoparticles. This work combines the effect of three parameters of the fluid $\emptyset, \gamma,$ and γ_T. The results showed that both velocity components decrease inside the boundary layer when ϕ *and* γ_T increase and slightly increase when γ values increase. The shear stress and temperature distribution of the fluid inside the layer decrease when ϕ increases while both increase when the other parameters increase. On the other hand, the heat flux increases only when ϕ values increase.

Nomenclature

Latin characters

x	vertical distance
y	horizontal distance from the plate
u	velocity component in x-direction
v	velocity component in y-direction
k	permeability coefficient
T	temperature of the fluid
T_c	Curie temperature
T_∞	temperature outside the boundary layer
H	the magnetic field strength
H_x, H_y	components of the magnetic field intensity
B_x, B_y	magnetic induction components
P_r	Prandtl number
K, Q	group coefficient function
a	group parameter

Greek characters

ν	kinematic viscosity of the fluid
μ_0	magnetic permittivity of vacuum
γ	magnetic field strength of the source
γ_T	temperature difference ratio with respect to ambient temperature $\gamma_T = \frac{\Delta T}{T_\infty}$
$\emptyset$	volume fraction
σ	fluid conductivity
ρ	fluid density
α	thermal diffusivity $\frac{\nu}{Pr}$

REFERENCES

1. Aly, A. M., & Ahmed, S. E. (2020). ISPH simulations for a variable magneto-convective flow of a ferrofluid in a closed space includes open circular pipes. *International Communications in Heat and Mass Transfer*, *110*, 104412.
2. Aminfar, H., Mohammadpourfard, M., & Mohseni, F. (2012). Two-phase mixture model simulation of the hydro-thermal behavior of an electrical conductive ferrofluid in the presence of magnetic fields. *Journal of Magnetism and Magnetic Materials*, *324*(5), 830-842.
3. Ghasemian, M., Ashrafi, Z. N., Goharkhah, M., & Ashjaee, M. (2015). Heat transfer characteristics of Fe3O4 ferrofluid flowing in a mini channel under constant and alternating magnetic fields. *Journal of Magnetism and Magnetic Materials*, *381*, 158-167.
4. Goshayeshi, H. R., Safaei, M. R., Goodarzi, M., & Dahari, M. (2016). Particle size and type effects on heat transfer enhancement of Ferro-nanofluids in a pulsating heat pipe. *Powder Technology*, *301*, 1218-1226.
5. Kassem, M. M., & Rashed, A. S. (2009). "Group similarity transformation of a time dependent chemical convective process", Proc. World Acad. Sci. Eng. Technol. Proceedings of World Academy of Science, *Engineering and Technology 40* (2009), 44-51.
6. Kassem, M. M., & Rashed, A. S. (2019). N-solitons and cuspon waves solutions of (2+ 1)-dimensional Broer–Kaup–Kupershmidt equations via hidden symmetries of Lie optimal system. *Chinese journal of physics*, *57*, 90-104.
7. Mabrouk, S. M., & Rashed, A. S. (2017). Analysis of (3+ 1)-dimensional Boiti–Leon–Manna–Pempinelli equation via Lax pair investigation and group transformation method. *Computers & Mathematics with Applications*, *74*(10), 2546-2556.
8. Mabrouk, S. M., & Rashed, A. S. (2019). N-Solitons, kink and periodic wave solutions for (3+ 1)-dimensional Hirota bilinear equation using three

distinct techniques. *Chinese Journal of Physics*, *60*, 48-60.
9. Mabrouk, S., & Kassem, M. (2014). Group similarity solutions of (2+ 1) Boiti-Leon-Manna-Pempinelli Lax pair. *Ain Shams Engineering Journal*, *5*(1), 227-235.
10. Mabrouk, S., Kassem, M., & Abd-el-Malek, M. (2013). Group similarity solutions of the lax pair for a generalized Hirota–Satsuma equation. *Applied Mathematics and Computation*, *219*(14), 7882-7890.
11. Majeed, A., Zeeshan, A., & Ellahi, R. (2016). Unsteady ferromagnetic liquid flow and heat transfer analysis over a stretching sheet with the effect of dipole and prescribed heat flux. *Journal of Molecular Liquids*, *223*, 528-533.
12. Monroe, J. G., Kumari, S., Fairley, J. D., Walters, K. B., Berg, M. J., & Thompson, S. M. (2019). On the energy harvesting and heat transfer ability of a ferro-nanofluid oscillating heat pipe. *International Journal of Heat and Mass Transfer*, *132*, 162-171.
13. Morgan, A. J. A. (1952). The reduction by one of the number of independent variables in some systems of partial differential equations. *The Quarterly Journal of Mathematics*, *3*(1), 250-259.
14. Nessab, W., Kahalerras, H., Fersadou, B., & Hammoudi, D. (2019). Numerical investigation of ferrofluid jet flow and convective heat transfer under the influence of magnetic sources. *Applied Thermal Engineering*, *150*, 271-284.
15. Pal, S., Datta, A., Sen, S., Mukhopdhyay, A., Bandopadhyay, K., & Ganguly, R. (2011). Characterization of a ferrofluid-based thermomagnetic pump for microfluidic applications. *Journal of Magnetism and Magnetic Materials*, *323*(21), 2701-2709.
16. Rashed, A. S. (2019). Analysis of (3+ 1)-dimensional unsteady gas flow using optimal system of Lie symmetries. *Mathematics and Computers in Simulation*, *156*, 327-346.
17. Rashed, A. S., & Kassem, M. M. (2008). Group analysis for natural convection from a vertical plate. *Journal of computational and applied mathematics*, *222*(2), 392-403.
18. Saleh, R., Kassem, M., & Mabrouk, S. (2017). Exact solutions of Calgero–Bogoyavlenskii–Schiff equation using the singular manifold method after Lie reductions. *Mathematical Methods in the Applied Sciences*, *40*(16), 5851-5862.
19. Sharifi, A., Motlagh, S. Y., & Badfar, H. (2019). Ferro hydro dynamic analysis of heat transfer and biomagnetic fluid flow in channel under the effect of two inclined permanent magnets. *Journal of Magnetism and Magnetic Materials*, *472*, 115-122.
20. Sheikholeslami, M., & Ganji, D. D. (2014). Ferrohydrodynamic and magnetohydrodynamic effects on ferrofluid flow and convective heat transfer. *Energy*, *75*, 400-410.
21. Sheikholeslami, M., Ganji, D. D., & Rashidi, M. M. (2015). Ferrofluid flow and heat transfer in a semi annulus enclosure in the presence of magnetic source considering thermal radiation. *Journal of the Taiwan Institute of Chemical Engineers*, *47*, 6-17.
22. Sheikholeslami, M., Vajravelu, K., & Rashidi, M. M. (2016). Forced convection heat transfer in a semi annulus under the influence of a variable magnetic field. *International journal of heat and mass transfer*, *92*, 339-348.
23. Sun, X. H., Massoudi, M., Aubry, N., Chen, Z. H., & Wu, W. T. (2019). Natural convection and anisotropic heat transfer in a ferro-nanofluid under magnetic field. *International Journal of Heat and Mass Transfer*, *133*, 581-595.